Organization and number of orexinergic neurons in the hypothalamus of two species of Cetartiodactyla: A comparison of giraffe (*Giraffa camelopardalis*) and harbour porpoise (*Phocoena phocoena*)

Leigh-Anne Dell [a], Nina Patzke [a], Adhil Bhagwandin [a,b], Faiza Bux [a], Kjell Fuxe [c], Grace Barber [b], Jerome M. Siegel [b], Paul R. Manger [a,*]

[a] School of Anatomical Sciences, Faculty of Health Sciences, University of the Witwatersrand, 7 York Road, Parktown 2193, Johannesburg, South Africa
[b] Department of Psychiatry, University of California, Los Angeles, Neurobiology Research 151A3, Sepulveda VAMC, 16111 Plummer St, North Hills, CA 91343, USA
[c] Department of Neuroscience, Karolinska Institutet, Retzius väg 8, S-171 77 Stockholm, Sweden

ABSTRACT

The present study describes the organization of the orexinergic (hypocretinergic) neurons in the hypothalamus of the giraffe and harbour porpoise – two members of the mammalian Order Cetartiodactyla which is comprised of the even-toed ungulates and the cetaceans as they share a monophyletic ancestry. Diencephalons from two sub-adult male giraffes and two adult male harbour porpoises were coronally sectioned and immunohistochemically stained for orexin-A. The staining revealed that the orexinergic neurons could be readily divided into two distinct neuronal types based on somal volume, area and length, these being the parvocellular and magnocellular orexin-A immunopositive (OxA+) groups. The magnocellular group could be further subdivided, on topological grounds, into three distinct clusters – a main cluster in the perifornical and lateral hypothalamus, a cluster associated with the zona incerta and a cluster associated with the optic tract. The parvocellular neurons were found in the medial hypothalamus, but could not be subdivided, rather they form a topologically amorphous cluster. The parvocellular cluster appears to be unique to the Cetartiodactyla as these neurons have not been described in other mammals to date, while the magnocellular nuclei appear to be homologous to similar nuclei described in other mammals. The overall size of both the parvocellular and magnocellular neurons (based on somal volume, area and length) were larger in the giraffe than the harbour porpoise, but the harbour porpoise had a higher number of both parvocellular and magnocellular orexinergic neurons than the giraffe despite both having a similar brain mass. The higher number of both parvocellular and magnocellular orexinergic neurons in the harbour porpoise may relate to the unusual sleep mechanisms in the cetaceans.

© 2012 Elsevier B.V. All rights reserved.

1. Introduction

The mammalian order Cetartiodactyla was originally considered to be two distinct orders: cetaceans (whales and dolphins)

and artiodactyla (even-toed ungulates). Extensive phylogenetic studies have made it possible to group all 290 extant species of cetaceans and artiodactyls into the order Cetartiodactyla (Price et al., 2005). This grouping allows for numerous comparative studies to be performed across species within a single mammalian order that are either aquatic carnivores (cetaceans) or terrestrial herbivores (artiodactyls) (Price et al., 2005). Modern morphological studies show that cetaceans and artiodactyls both share a common Condylarthran ancestry (O'Leary, 1999), while modern molecular studies have identified a paraphyletic artiodactyla order with cetaceans nested within as a sister taxa to the Hippopotamidae (Shimamura et al., 1997).

The giraffe, *Giraffa camelopardalis*, is the tallest extant terrestrial mammal and is characterised by its phenotypically unique long neck (Badlangana et al., 2009) that creates many challenges for its physiology. Giraffes are reported to require a small amount of sleep that appears to be constituted by many short bouts, totalling less

than an average of 5 h per night (Tobler and Schwierin, 1996). Recent neuroanatomical studies of the giraffe have examined aspects of the corticospinal tract, diencephalon and the brainstem (Badlangana et al., 2007a,b; Bux et al., 2010), but to date no previous study has examined the orexinergic system, although reports on this system in the sheep and pig have been provided (Iqbal et al., 2001; Ettrup et al., 2010). While a great deal of work has focussed on the neuroanatomy of the cetaceans (e.g. Hof et al., 2005; Manger, 2006; Hof and Van der Gucht, 2007; Oelschlager, 2008) very little has focussed on neural systems related to their sleep-wake cycle and hypothalamus of cetaceans (Manger et al., 2003, 2004; reviewed in Lyamin et al., 2008). Indeed, given the unusual unihemispheric slow wave sleep observed in cetaceans (Lyamin et al., 2008), it is of broad interest to the understanding of mammalian sleep to examine the neural systems implicated in regulation of the sleep-wake cycle in cetaceans, one such system being the orexinergic system.

Orexinergic neurons are found in the diencephalon (Peyron et al., 1998) and have been documented in the hypothalamus of several mammalian species (e.g. Kruger et al., 2010). The orexinergic system is implicated in the regulation of blood pressure, neuroendocrine functions, body temperature, the sleep-wake cycle, stimulation of food intake, increased arousal, energy homeostasis and locomotor activity (e.g. Peyron et al., 1998; Wagner et al., 2000; McGranaghan and Piggins, 2001; Fabris et al., 2004; Baumann and Bassetti, 2005; Spinazzi et al., 2006; McGregor et al., 2011). The present study provides a comparison of the nuclear organization of the orexinergic system in the hypothalamus of the giraffe and the harbour porpoise by means of immunohistochemical staining. To accurately access the number of orexinergic neurons in the hypothalamus of the giraffe and harbour porpoise, rigorous stereological counting techniques were employed.

2. Materials and methods

Brains from two sub-adult male giraffes (G. camelopardalis) (body mass 480 kg and brain mass of 544 g, body mass 450 kg and brain mass of 509 g) and two adult male harbour porpoises (Phocoena phocoena) (body mass 49 kg and brain mass of 503 g, body mass 55 kg and brain mass of 486 g) were used in the current study. All animals were treated and used according to the guidelines of the University of Witwatersrand Animal Ethics Committee which correspond with those of the NIH for care and use of animals in scientific experimentation. Both giraffes were euthanized with an intravenous overdose of sodium pentobarbital in the late afternoon after being used for unrelated physiological studies. Following euthanasia the heads were removed from the body at the level of the third cervical vertebrae, the common carotid arteries located and a 4 mm inner diameter cannula inserted and secured in place. The heads were then gravity perfused initially with a 10 l rinse of 0.9% saline solution at a temperature of 4 °C followed by 10 l of 4% paraformaldehyde in 0.1 M PB at a temperature of 4 °C for fixation (as per the method described in Manger et al., 2009). Both harbour porpoises were obtained after being killed according to Greenlandic cultural practices and perfused via the heart with an initial rinse of 20 l of 0.9% saline solution at a temperature of 4 °C followed by 20 l of 4% paraformaldehyde in 0.1 M PB. The brains were removed from the skull and post-fixed in 4% paraformaldehyde in 0.1 M PB (24 h at 4 °C) and allowed to equilibrate in 30% sucrose in 0.1 M PB. The brains were dissected and the diencephalon frozen in crushed dry ice and coronal sections of 50 μm thickness were made using a sliding microtome.

A one in three series were stained for Nissl, myelin and orexin A. Nissl sections were mounted on 0.5% gelatine coated glass slides and then cleared in a solution of 1:1 chloroform and 100% alcohol overnight, after which the sections were then stained with 1% cresyl violet. The myelin series sections were refrigerated for two weeks in 5% formalin then mounted on 1.5% gelatine coated slides and stained with a modified silver stain (Gallyas, 1979).

The sections used for immunohistochemistry were initially treated for 30 min with an endogenous peroxidase inhibitor (49.2% methanol:49.2% 0.1 M PB:1.6% of 30% H₂O₂), followed by three 10 min rinses in 0.1 M PB. The sections were then preincubated at room temperature for 2 h in a blocking buffer solution containing 3% normal serum (NGS, Chemicon/Millipore), 2% bovine serum albumin (BSA, Sigma) and 0.25% Triton X-100 (Merck) in 0.1 M PB. The sections were then placed in a primary antibody solution (blocking buffer with correctly diluted primary antibody) and incubated at 4 °C for 48 h under gentle shaking. To reveal orexinergic/hypocretinergic

neurons, anti-orexin A (AB3704, Chemicon/Millipore, raised in rabbit, against a synthetic peptide corresponding to the C-terminal portion of the bovine Orexin-A peptide) was used at a dilution of 1:2000. This was followed by three 10 min rinses in 0.1 M PB, after which the sections were incubated in a secondary antibody solution for 2 h at room temperature.

The secondary antibody solution contained a 1:1000 dilution of biotinylated anti-rabbit IgG (BA-1000, Vector Labs) in a blocking buffer solution containing 3% NGS and 2% BSA in 0.1 M PB. This was followed by three 10 min rinses in 0.1 M PB after which the sections were incubated in AB solution (Vector Labs) for 1 h. After three further 10 min rinses in 0.1 M PB, the sections were placed in a solution of 0.05% 3,3′-diaminobenzidine (DAB) in 0.1 M PB for 5 min (2 ml/section), followed by the addition of 3 μl of 30% H₂O₂ to each 1 ml of solution in which each section was immersed. Chromatic precipitation of the sections was monitored visually under a low power stereomicroscope. This process was allowed to continue until the background staining of the sections was appropriate enough to assist with architectonic reconstruction without obscuring any immunopositive neurons. The precipitation process was stopped by immersing the sections in 0.1 M PB and then rinsing them twice more in 0.1 M PB. Omission of the primary or secondary antibody in selected sections was employed as negative controls, for which no staining was evident. In addition to these negative controls that eliminated the possibility of parasitic background staining we ran an additional antibody and peptide inhibition assay, as the novel findings of parvocellular orexinergic neurons in the medial hypothalamus of the giraffe and harbour porpoise needed to be verified. We used an additional orexin-A antibody available from Millipore (AB3098, raised in rabbit, against an 18 amino acid peptide mapping near the amino terminus of mouse Orexin-A) at a dilution of 1:2000 as per the protocol described above. The reason a different antibody was used is due to the fact that no specific inhibition peptide is available for the orexin-A antibody AB3704. The orexin control peptide (AG774, Millipore, specifically for AB3098) was used at a dilution of 1 mg/ml in the primary antibody solution (see above). This solution was incubated for 3 h at 4 °C prior to being used on the sections. In the case of the AB3098 orexin-A antibody, neurons were observed in the hypothalamus of both the giraffe and harbour porpoise and showed an identical staining pattern to that seen with the AB3704 orexin-A antibody. In the sections where the primary antibody (AB3098) had been inhibited, no staining was evident in either the parvocellular or magnocellular orexinergic regions.

The immunohistochemically stained sections were mounted on 0.5% gelatine coated slides and left to dry overnight. The sections were then dehydrated in graded series of alcohols, cleared in xylene and cover slipped with Depex. All sections were examined under low power using a stereomicroscope and the architectonic borders of the sections were traced according to the Nissl and myelin stained sections using a camera lucida. The immunostained sections were then matched to the traced drawings, adjusted slightly for any differential shrinking of the stained sections and immunopositive neurons were marked. The drawings were then scanned and redrawn using the Canvas 8 (Deneba) drawing program.

The number of orexinergic (OxA+) positive cells was determined with stereological techniques through the complete hypothalamus in all 4 brains. A Nikon E600 microscope with three axis motorized stage, video camera, Neurolucida interface and Stereo-Investigator software (MicroBrightfield Corp.) was used for the stereological counts. In an attempt to achieve the most accurate estimation of OxA+ neurons, a pilot study was first conducted in an individual of each species. The pilot study determined the best counting frame size and grid size and these parameters were then used for all individuals of each species investigated. A 200 μm × 186 μm counting frame and a 1259 μm × 1220 μm sampling grid were employed in each individual (Table 1). Only orexinergic neurons with clearly visible nuclei were marked in the sampling grids. For the calculation of total neuron numbers, we measured section thickness in a random sample of 20 sections from each individual in the regions where orexinergic neurons were present and used these measurements to calculate the species average mounted thickness. The 'optical fractionator probe' function of the software computationally determined the number of parvocellular OxA+ cells, the number of magnocellular OxA+ cells and the total number of OxA+ in the hypothalamus of each individual using the following formula:

$$N = \frac{Q}{\text{SSF} \times \text{ASF} \times \text{TSF}}$$

where N – was the total estimated neuronal number, Q – was the number of neurons counted, SSF – was the section sampling fraction (in the current study this was 0.5), ASF – is the area sub fraction (this was the ratio of the size of the counting frame to the size of the sampling grid), and TSF – was the thickness sub fraction (this was the ratio of the dissector height relative to cut section thickness). In order to determine TSF we used the average mounted section thickness calculated for each individual (Table 1), subtracted the total vertical guard zones (10 μm) to give dissector height and used the ratio of dissector height to cut section thickness (50 μm) to provide TSF for each individual. A function in the stereology programme called the "nucleator probe" facilitated the estimation of the mean cross-sectional area, volume and length of the orexinergic positive cells. Only neurons with a distinct nucleus were chosen for analysis. The "nucleator probe" was employed in conjunction with the optical fractionator and stereology procedures for systematic random sampling to identify cells (Gundersen, 1988). In total, seven probes were

Table 1
Stereological parameters used for *Giraffa camelopardalis* and *Phocoena phocoena*.

Animal ID	Counting frame size (μm)	Sampling grid size (μm)	Cut thickness (μm)	Average mounted thickness (μm)	Vertical guard zones (top and bottom, μm)	Section interval	Number of sampling sites	Average CE (Gunders, $m = 0$)	Average CE (Gunders, $m = 1$)
Giraffa camelopardalis									
GC1	$200 \times 186 \times 12$	1259×1220	50	19.18	5	4	497	0.09	0.09
GC2	$200 \times 186 \times 12$	1259×1220	40	21.74	5	4	699	0.12	0.10
Phocoena phocoena									
PP1	$200 \times 186 \times 15$	1259×1220	50	27.32	5	10	451	0.09	0.09
PP2	$200 \times 186 \times 15$	1259×1220	50	20.52	5	10	336	0.12	0.10

used in the current study namely: the optical fractionators, optical fractionator using number weighted section thickness, physical dissector, physical fractionator, Schmitz nearest neighbour, Cavalieri estimator for area and volume, and combination of planes with the optical fractionator for absolute length. As a measure of variability, the standard deviations/error (SD/SE) together with the mean values were given. In the present study, a permutation *t*-test (10 000 permutations) was used for all reasonable paired comparisons of volume, area and length; corrected for multiple tests using the sequential Bonferroni method (Holm, 1979). Additionally, counts were tested using the following equation:

$$t_{\alpha[\infty]} = \frac{Y_1 - Y_2}{\sqrt{Y_1 + Y_2}}$$

against the *t*-distribution, where Y_1 is the first count and Y_2 is the second count (Sokal and Rohlf, 1998). Signficance values were adjusted again using the sequential Bonferroni method. Statistically significant differences were considered at $\alpha = 0.05$.

3. Results

Orexinergic neurons in the hypothalamus of the giraffe and the harbour porpoise were visualized by means of immunohistochemical methods. In both species numerous orexin A immunoreactive neurons (OxA+) were found within the hypothalamus and in closely adjacent areas. These neurons could be readily distinguished into two distinct neuronal types based on somal size (volume, area and length), these being the parvocellular and magnocellular OxA+ groups. The magnocellular group could be further subdivided into three distinct nuclei, a main cluster in the perifornical and lateral hypothalamus, a cluster associated with the zona incerta and a cluster associated with the optic tract. The parvocellular neurons were found in the medial hypothalamus, but could not be subdivided into separate nuclei, rather forming a topologically continuous cluster. The parvocellular cluster appears to be unique to the Cetartiodactyla as these neurons have not been described in other mammals to date, while the magnocellular nuclei appear to be homologous to similar nuclei described in other mammals. For both parvocellular, magnocellular and mean orexinergic somal numbers, the values are higher for the harbour porpoise than the giraffe. In contrast to this all aspects of somal size (volume, area and length) of the orexinergic neurons of the giraffe are larger than those of the harbour porpoise.
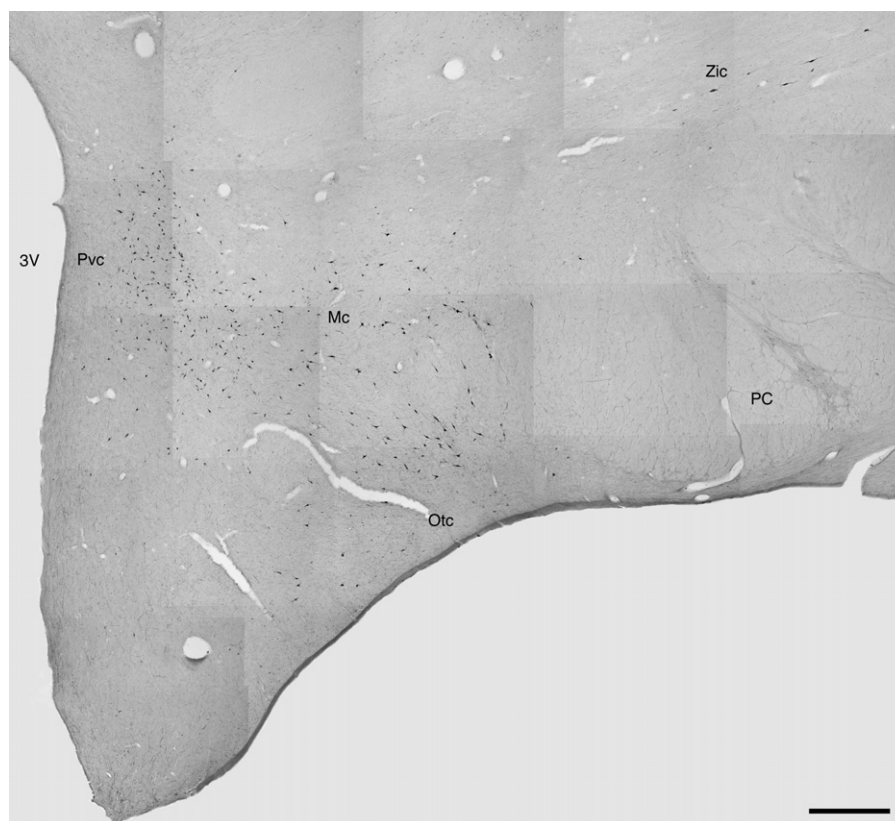

Fig. 1. Photomicrographic montage demonstrating the location of orexin-A immunoreactive neurons within the hypothalamus of the giraffe showing the distinct magnocellular neurons as the main cluster (Mc), the zona incerta cluster (Zic) and the optic tract cluster (Otc) and the parvocellular neurons (Pvc) as a cluster in the medial hypothalamus. Medial is to the left, dorsal to the top. Scale bar = 1 mm. 3V – third ventricle; PC – cerebral peduncle.

3.1. Orexinergic neurons of the giraffe

3.1.1. Parvocellular cluster

In the giraffe, the parvocellular OxA+ group was located in the medial zone of the hypothalamus between the wall of the third ventricle and the fornix, mainly in a paraventricular position (Figs. 1 and 2A). Anteriorly, these OxA+ neurons were found in the ventromedial aspect of the hypothalamus and posteriorly these neurons were located throughout the dorsoventral extent of the hypothalamus, but mostly within the dorsal region (Fig. 3B–E). The parvocellular OxA+ neurons were found in a moderate to high density throughout the regions in which they were localized and no distinct topological discontinuities were observed, thus they appear to form a single cluster extending as a column along the rostro-caudal axis of the hypothalamus. The somal bodies were ovoid in shape and the majority of the neurons were clearly bipolar and showed no specific dendritic orientation lying in a moderately dense plexus of OxA+ varicose nerve terminals.

3.1.2. Magnocellular clusters

Magnocellular OxA+ neurons in the giraffe were observed throughout the entire lateral zone of the hypothalamus, this being the region of the hypothalamus lateral to the fornix and are termed the main cluster (Figs. 1, 2B and 3). At the anterior level of the hypothalamus, some OxA+ neurons were found in a far lateral position above the optic tract, these neurons forming the optic tract cluster (Fig. 3A–C). Dorsally, at the mid-level of the hypothalamus a small number of OxA+ neurons were found within the zona incerta and the very proximal part of the reticular nucleus, these neurons forming the zona incerta cluster (Figs. 2C and 3B–D). The magnocellular OxA+ neurons were found in a moderate density throughout the regions in which they were localized, having few OxA+ nerve terminals and they appeared significantly larger than the neurons of the above described parvocellular OxA+ group through visual inspection (also see stereological analysis provided below). The magnocellular OxA+ neurons exhibited a variety of somal shapes with some being bipolar while the majority appeared multipolar. No clear dendritic orientation was observed in the main and optic tract neuronal clusters, but the OxA+ neurons found in the zona incerta were clearly bipolar and exhibited a dendritic orientation coincident with the mediolateral orientation of the reticular nucleus.

3.2. Orexinergic neurons of the harbour porpoise

3.2.1. Parvocellular cluster

In the harbour porpoise, the parvocellular OxA+ cells were distributed in the medial zone of the hypothalamus mainly in a paraventricular region, failing to invade the periventricular zone of the third ventricle and lying in a plexus of varicose OxA+ nerve terminals of high density (Figs. 4, 5B and 6). The cells extend anteriorly in a ventromedial orientation and posteriorly in a dorsomedial orientation. A few cells were located adjacent to the superior border of the third ventricle. The parvocellular OxA+ cells appeared present in a moderate to high cell density throughout the regions in which they were localized and no distinct topological discontinuities were observed, thus they appear to form a single cluster extending as a column along the rostro-caudal axis of the medial hypothalamus. The somal bodies were round in shape and the majority of the neurons were unipolar but many were bipolar. None of these neurons showed any specific dendritic orientation.

3.2.2. Magnocellular clusters

The magnocellular OxA+ neurons in the harbour porpoise were identified throughout the hypothalamus, lateral to the parvocellular neurons, in a location lateral to the fornix, occupying the
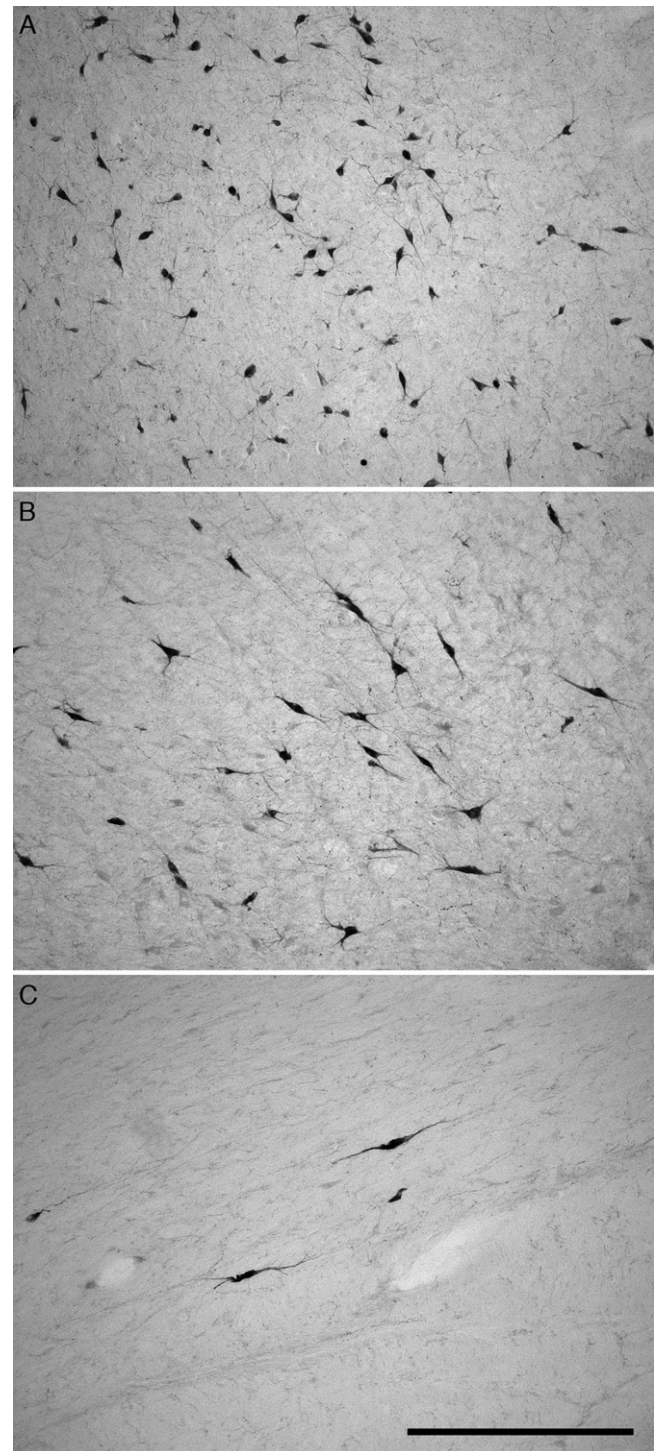
Fig. 2. Photomicrographs illustrating the neuronal morphological differences between the magnocellular and parvocellular clusters of orexin-A immunoreactive nuclear groups within the hypothalamus of the giraffe. (A) Orexin-A immunoreactive neurons of the parvocellular cluster in the medial hypothalamus. (B) Orexin-A immunoreactive neurons of the magnocellular main cluster in the perifornical region. (C) Orexin-A immunoreactive neurons of the magnocellular zona incerta cluster in the lateral hypothalamic area. In all images, medial is to the left and dorsal to the top. Scale bar in C = 500 μm and applies to all.

entire lateral zone of the hypothalamus forming the main cluster (Figs. 4, 5B and 6). These neurons were observed to be of high density and embedded in a OxA+ nerve terminal plexus of high density. Anteriorly within the hypothalamus, there were a significant number of OxA+ neurons extending well into the optic
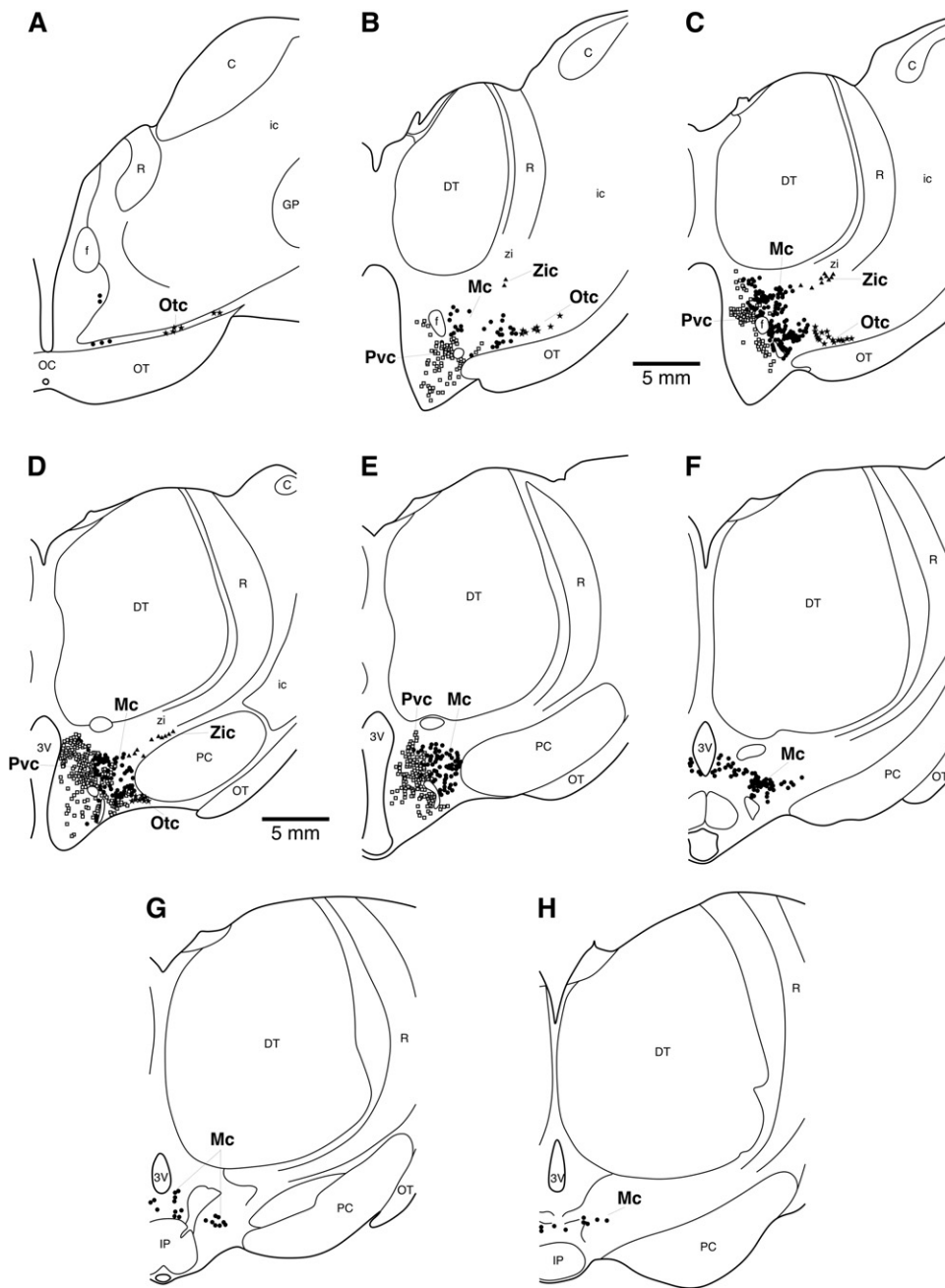
Fig. 3. Drawings of coronal sections through one half of the giraffe diencephalon illustrating orexin-A immunoreactive neuron distribution. A single black dot indicates a single magnocellular orexinergic neuron while a single open square represents a single parvocellular orexinergic neuron. Drawing A represents the most rostral section, H the most caudal, and each drawing is approximately 500 μm apart. In all drawings, medial is to the left and dorsal to the top. See list for abbreviations.

tract region forming the optic tract cluster (Fig. 6F–L). Some neurons were also identified within the mid level of the hypothalamus, occupying the proximal part of the zona incerta forming the low density zona incerta cluster located in a region having a low density of OxA+ nerve terminals (Figs. 5C and 6). The magnocellular OxA+ cell density in the main cluster was considered moderate to high and the distribution pattern was more clustered and dense than that of the parvocellular OxA+ neurons. The magnocellular OxA+ neurons appeared to have an ovoid somal shape and exhibited a combination of bipolar and multipolar types. Although no clear dendritic orientation was noted, the cells within the zona incerta cluster were all bipolar and exhibited a dendritic orientation coincident with that of the reticular nucleus, as seen in the giraffe.

3.3. Stereological analysis of orexinergic neuronal numbers and sizes

Stereological counts of OxA+ cell bodies in the giraffe revealed a mean of 7676 ± 128 s.e. for the parvocellular cluster, 7327 ± 177 for the magnocellular clusters and $15\,003 \pm 305$ for the total estimated OxA+ cell bodies (Fig. 7, Table 2). Counts from the harbour porpoise revealed a mean of $10\,834 \pm 282$ for the parvocellular cluster and $10\,419 \pm 914$ for the magnocellular clusters and $21\,254 \pm 1186$ for the total estimated OxA+ cell bodies (Fig. 7 and Table 2). When comparing neuronal numbers between the two giraffe sampled, no significant differences were noted when comparing numbers from GC1 and GC2 for the parvocellular or magnocellular groups; however, a comparison of total orexinergic neuron number revealed that GC2 had significantly more neurons than GC1 ($p = 0.008$). A similar
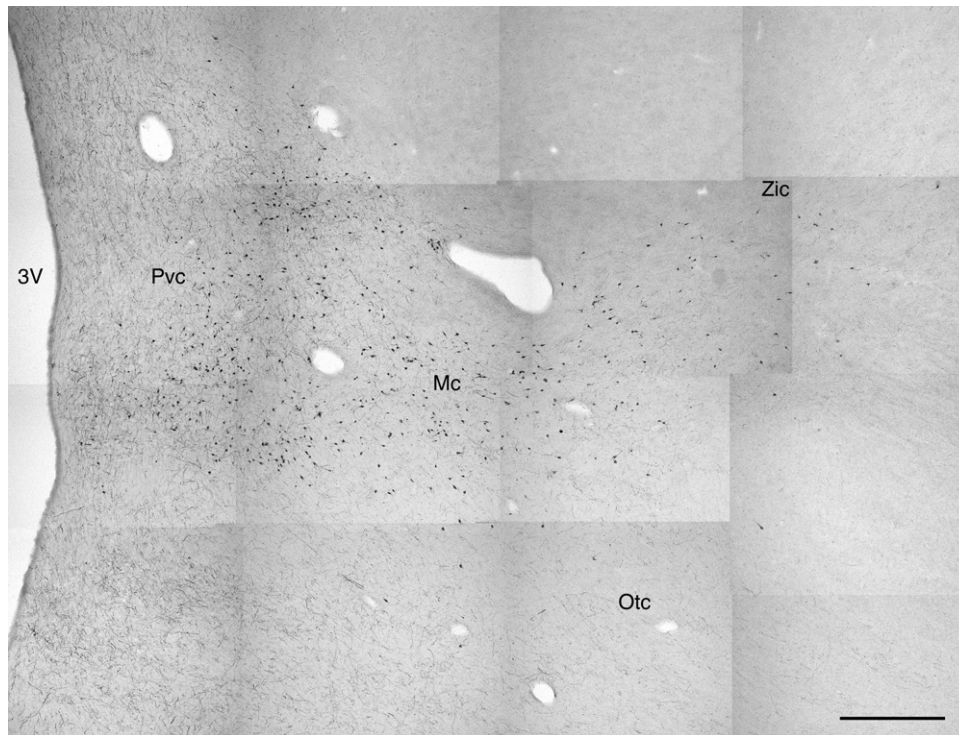
Fig. 4. Photomicrographic montage demonstrating the location of orexin-A immunoreactive neurons within the hypothalamus of the harbour porpoise showing the distinct magnocellular neurons as the main cluster (Mc), the zona incerta cluster (Zic) and the optic tract cluster (Otc) and the parvocellular neurons (Pvc) as a cluster in the medial hypothalamus. Medial is to the left, dorsal to the top. Scale bar = 1 mm. 3V – third ventricle.

comparison within the harbour porpoises studied revealed that PP2 had significantly more parvocellular ($p = 0.004$), magnocellular ($p = 1.864 \times 10^{-35}$) and total neuronal numbers ($p = 2.373 \times 10^{-29}$) than PP1. Comparing neuronal numbers between species, it was clear that GC1 had significantly lower numbers of parvocellular neurons than PP1 ($p = 6.408 \times 10^{-110}$) and PP2 ($p = 1.950 \times 10^{-148}$), as did GC2 (GC2 vs PP1 – $p = 8.214 \times 10^{-91}$; GC2 vs PP2 – $p = 3.767 \times 10^{-126}$). A similar situation was observed for the magnocellular orexinergic neuronal numbers where the giraffe had less magnocellular neurons than the harbour porpoise (GC1 vs PP1 – $p = 3.387 \times 10^{-73}$; GC1 vs PP2 – $p = 1.287 \times 10^{-206}$; GC2 vs PP1 – $p = 6.372 \times 10^{-52}$; GC2 vs PP2 – $p = 5.097 \times 10^{-170}$). Lastly, the total numbers of orexinergic neurons in the brain of the giraffes were significantly less than those observed in the brains of the harbour porpoises (GC1 vs PP1 – $p = 3.297 \times 10^{-181}$; GC1 vs PP2 – $p = 0.000$; GC2 vs PP1 – $p = 4.780 \times 10^{-140}$; GC2 vs PP2 – $p = 1.203 \times 10^{-293}$).

Stereological estimation of the volume of an OxA+ cell body in the giraffe presented a weighted mean of 3072.6 ± 82.2 s.e. μm^3 for the parvocellular neurons and 8704.5 ± 340.7 μm^3 for the magnocellular neurons (Figs. 7 and 8, Table 2). For the harbour porpoise the volume of the OxA+ neurons presented a weighted mean of 2399.4 ± 74.0 s.e. μm^3 for the parvocellular neurons and 7207.0 ± 250.9 μm^3 for the magnocellular neurons (Figs. 7 and 8, Table 2). Statistically significant differences were noted: (1) within the giraffe, where the magnocellular neurons had a higher mean volume than the parvocellular neurons (GC1mag vs GC1par – $p = 0.000$; GC2mag vs GC2par – $p = 0.000$); and (2) within the harbour porpoise, where the magnocellular neurons had a higher mean volume than the parvocellular neurons (PP1mag vs PP1par – $p = 0.000$; PP2mag vs PP2par – $p = 0.000$). These comparisons show that within both species, the parvocellular orexinergic neurons are significantly smaller than the magnocellular neurons. When comparing between species, it was noted that the magnocellular neurons of the giraffe were generally larger than those of the magnocellular

neurons of the harbour porpoise (GC1mag vs PP1mag – $p = 0.004$; GC1mag vs PP2mag – $p = 0.316$; GC2mag vs PP1mag – $p = 0.000$; GC2mag vs PP2mag – $p = 0.246$), with a similar situation being observed when comparing the parvocellular neurons between species (GC1par vs PP1par – $p = 0.000$; GC1par vs PP2par – $p = 0.481$; GC2par vs PP1par – $p = 0.000$; GC2par vs PP2par – $p = 0.002$).

Stereological estimation of the area of an OxA+ cell body in the giraffe presented a weighted mean of 246.1 ± 4.3 s.e. μm^2 for the parvocellular neurons and 480.4 ± 11.3 μm^2 for the magnocellular neurons (Figs. 7 and 8, Table 2). In the harbour porpoise a weighted mean of 210.0 ± 4.2 μm^2 was found for the parvocellular neurons and 432.3 ± 9.4 μm^2 for the magnocellular neurons (Figs. 7 and 8, Table 2). Statistically significant differences were noted: (1) within the giraffe, where the magnocellular neurons had a higher mean area than the parvocellular neurons (GC1mag vs GC1par – $p = 0.000$; GC2mag vs GC2par – $p = 0.000$); and (2) within the harbour porpoise, where the magnocellular neurons had a higher mean area than the parvocellular neurons (PP1mag vs PP1par – $p = 0.000$; PP2mag vs PP2par – $p = 0.000$). These comparisons show that within both species, the parvocellular orexinergic neurons are significantly smaller in area than the magnocellular neurons. When comparing between species, it was noted that the magnocellular neurons of the giraffe were generally larger in area than those of the magnocellular neurons of the harbour porpoise (GC1mag vs PP1mag – $p = 0.012$; GC1mag vs PP2mag – $p = 0.106$; GC2mag vs PP1mag – $p = 0.000$; GC2mag vs PP2mag – $p = 0.323$), with a similar situation being observed when comparing the parvocellular neuronal area between species (GC1par vs PP1par – $p = 0.000$; GC1par vs PP2par – $p = p = 0.463$; GC2par vs PP1par – $p = 0.000$; GC2par vs PP2par – $p = 0.002$).

Stereological estimation of the length of an OxA+ cell body in the giraffe presented a weighted mean of 8.7 ± 0.08 s.e. μm for the parvocellular neurons and 12.0 ± 0.13 μm for the magnocellular neurons (Figs. 7 and 8, Table 2). In the harbour porpoise a weighted
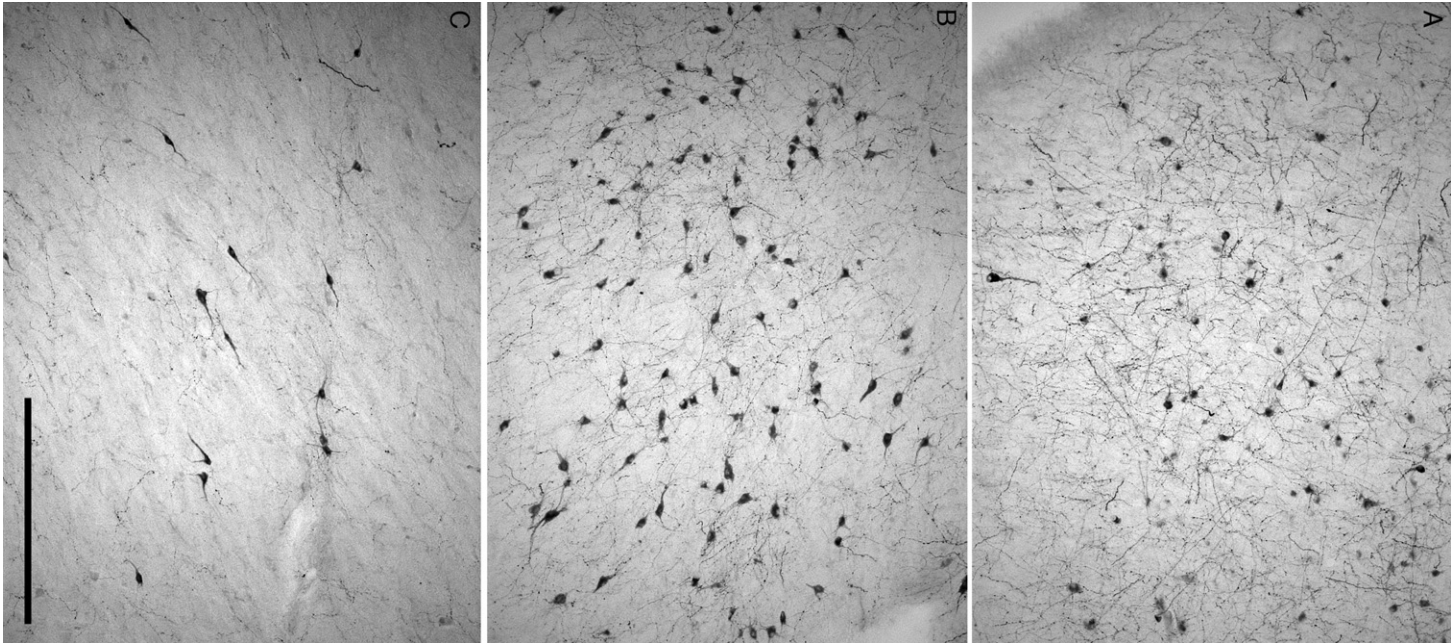
Fig. 5. Photomicrographs illustrating the neuronal morphological differences between the magnocellular and parvocellular clusters of orexin-A immunoreactive nuclear groups within the hypothalamus of the harbour porpoise. (A) Orexin-A immunoreactive neurons of the parvocellular cluster in the medial hypothalamus. (B) Orexin-A immunoreactive neurons of the magnocellular main cluster in the perifornical region. (C) Orexin-A immunoreactive neurons of the magnocellular zona incerta cluster in the lateral hypothalamic area. In all images medial is to the left and dorsal to the top. Scale bar in C = 500 μm and applies to all.

mean of 8.0 ± 0.08 μm was observed for the parvocellular neuron and 11.5 ± 0.13 μm for the magnocellular neurons (Figs. 7, 8, Table 2). Statistically significant differences were noted: (1) within the giraffe, where the magnocellular neurons had a greater mean length compared to the parvocellular neurons (GC1mag vs

Table 2
Table presenting data for individuals of *Giraffa camelopardalis* and *Phocoena phocoena* and the respective weighted means for estimated parvocellular cell counts, estimated magnocellular cell counts, estimated total cell counts, average estimated volume, average estimated cell area and average estimated cell length and standard errors.

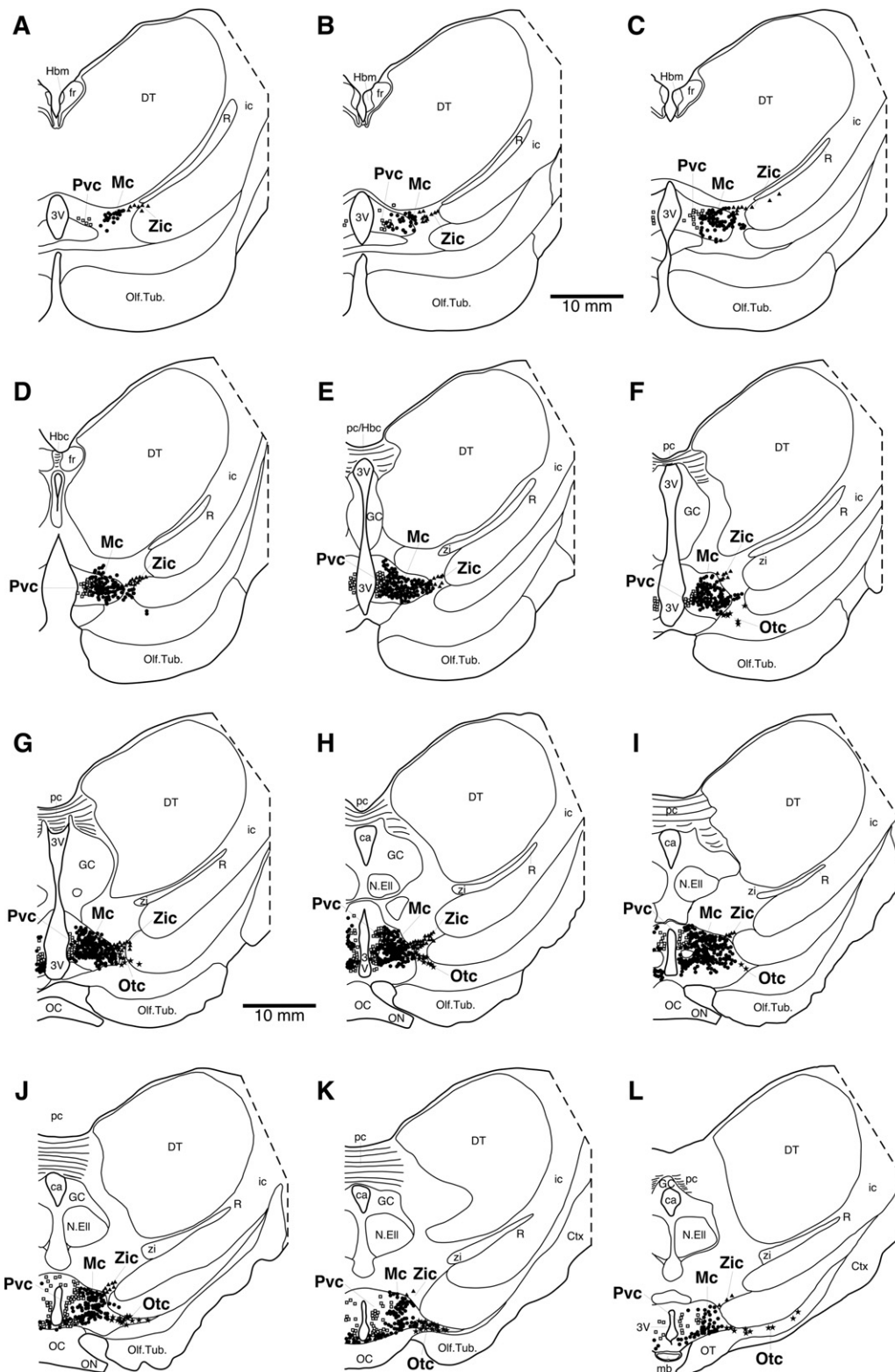| Animal ID	Sex	Body mass (kg)	Brain mass (g)	Estimated parvo	Estimated magno	Estimated total cell counts	Average estimated cell volume (μm³)		Average estimated cell area (μm²)		Average estimated cell length (μm)	
							Parvo	Magno	Parvo	Magno	Parvo	Magno
Giraffa camelopardalis												
GC1	M	480	544	7547	7150	14 698	2810.7	7987.8	232.8	451.0	8.5	11.6
GC2	M	450	509	7804	7504	15 309	3449.5	9735.8	265.2	522.7	9.0	12.6
Mean/weighted mean		465	526.5	7676 ± 128	7327 ± 177	15 003 ± 305	3072.6 ± 82.2	8704.5 ± 340.7	246.1 ± 4.3	480.4 ± 11.3	8.7 ± 0.08	12.0 ± 0.13
Phocena phocoena												
PP1	M	49	503	10 562	9606	20 068	2071.6	6081.3	190.6	386.8	7.7	10.9
PP2	M	55	486	11 106	11 333	22 439	2727.3	8332.8	229.4	477.8	8.4	12.1
Mean/weighted mean		52	494.5	10 834 272	10 419 914	21 254 1186	2399.4 74.0	7207.0 250.9	210.0 4.2	432.3 9.7	8.0 0.08	11.5 0.13

Fig. 6. Drawings of coronal sections through one half of the harbour porpoise diencephalon illustrating orexin-A immunoreactive neuron distribution. A single black dot indicates a single magnocellular orexinergic neuron while a single open square represents a single parvocellular orexinergic neuron. Drawing A represents the most rostral section, L the most caudal, and each drawing is approximately 500 μm apart. In all drawings, medial is to the left and dorsal to the top. See list for abbreviations.

GC1par – $p = 0.000$; GC2mag vs GC2par – $p = 0.000$); and (2) within the harbour porpoise, where the magnocellular neurons had a greater mean length compared to the parvocellular neurons (PP1mag vs PP1par – $p = 0.000$; PP2mag vs PP2par – $p = 0.000$). These comparisons show that within both species, the parvocellular orexinergic

neurons are significantly shorter in length than the magnocellular neurons. When comparing between species, it was noted that the magnocellular neurons of the giraffe were generally longer than those of the magnocellular neurons of the harbour porpoise (GC1mag vs PP1mag – $p = 0.028$; GC1mag vs PP2mag – $p = 0.234$; GC2mag vs
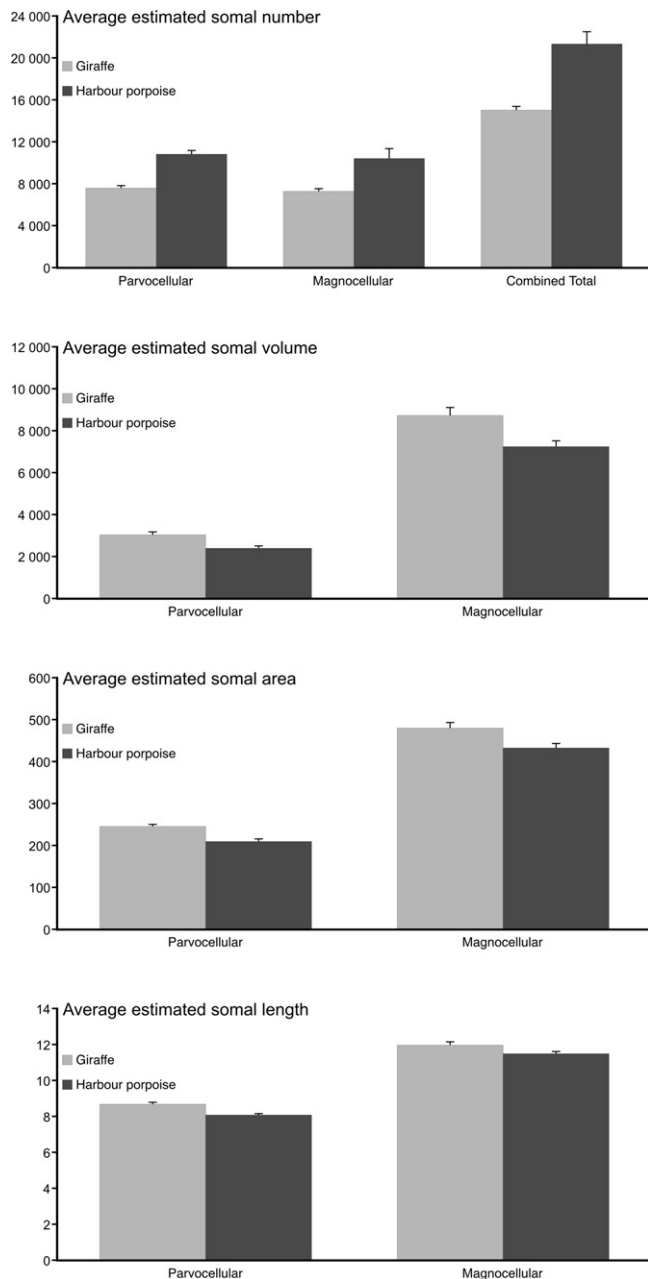
Fig. 7. Graphs showing the various parameters of stereological data for orexinergic immunopositive neurons in *Giraffa camelopardalis* (Gc, giraffe) and *Phocoena phocoena* (Pp, harbour porpoise). The graphs indicate average estimated values for orexinergic somal number, volume, area and length. Note that for both parvocellular (parvo), magnocellular (magno) and mean orexinergic somal numbers, the values are higher for the harbour porpoise than the giraffe. In contrast to this all aspects of somal size (volume, area and length) of the orexinergic neurons of the giraffe are larger than those of the harbour porpoise.

PP1mag – $p = 0.000$; GC2mag vs PP2mag – $p = 0.460$), with a similar situation being observed when comparing the parvocellular neuronal length between species (GC1par vs PP1par – $p = 0.000$; GC1par vs PP2par – $p = 0.396$; GC2par vs PP1par – $p = 0.000$; GC2par vs PP2par – $p = 0.005$).

4. Discussion

The present study aimed to determine the nuclear organisation and other morphological and quantitative features of the orexinergic system within the hypothalamus of giraffes and

harbour porpoises so that data concerning this arousal system in the Cetartiodactyla order could be generated. The giraffe and harbour porpoise both exhibited the same nuclear organisation of the orexinergic system, with both species displaying a novel parvocellular cluster of orexinergic neurons within the paraventricular zone of the hypothalamus and three magnocellular clusters lateral and dorsal to the fornix that appear homologous to similar clusters seen in other mammals. Stereological analysis confirmed the size differences of the parvocellular and magnocellular orexinergic neurons, and also demonstrated that the orexinergic neurons (both parvo and magno) found in the giraffe hypothalamus were larger (volume, area and length) than those observed in the harbour porpoise hypothalamus. The stereological analysis also indicates that the number of orexinergic neurons within the hypothalamus of the harbour porpoise (parvo, magno and total) was higher than that observed in the giraffe, despite both species having brain masses close to 500 g.

4.1. Nuclear organization of the orexinergic system in cetartiodactyla: comparison to other mammals

One of the novel findings within the current study was the observation of a significant parvocellular cluster of orexinergic neurons within the medial hypothalamic zone. This parvocellular cluster was observed in both the giraffe and harbour porpoise, indicating it to potentially be a Cetartiodactyla order specific feature (Manger, 2005). Our stereological analysis of cell size confirms the topological segregation of the orexinergic neurons and the smaller cell size of these neurons. To date the existence of parvocellular orexinergic neurons has not been reported in other artiodactyls; however, inspection of the photomicrographs published for both sheep (Iqbal et al., 2001) and the Gottingen mini-pig (Ettrup et al., 2010) indicate the presence of a similar parvocellular cluster, underlining the Cetartiodactyla specificity of this cluster. In no other mammals studied has such a cluster been reported (e.g. Kruger et al., 2010), but Nixon and Smale (2007) do note the occasional small orexinergic neuron in the medial hypothalamus of rats. Our own studies, using similar fixation processes and the same antibody have also not revealed this parvocellular cluster of orexinergic neurons in the microchiroptera, mole rats or rock hyraxes (Kruger et al., 2010; Bhagwandin et al., 2011a,b; Gravett et al., 2011).

In the current study three magnocellular clusters of orexinergic neurons were observed, these being the main cluster in the perifornical and lateral hypothalamic region, the zona incerta cluster extending from the lateral hypothalamus towards and mingling with the medial aspect of the zona incerta, and the optic tract cluster located in the ventral lateral hypothalamus just above the optic tract. These three clusters have been observed in the hypothalamus of most mammals studied to date and appear to form the basis of the mammalian orexinergic system. The only exception to this general pattern previously reported is the lack of the optic tract cluster in hamsters (Mintz et al., 2001 – Syrian hamster; McGranaghan and Piggins, 2001 – Syrian and Siberian hamsters; Khorooshi and Klingenspor, 2005 – Djungarian hamster; Vidal et al., 2005 – Golden hamster) and microchiroptera (Kruger et al., 2010). It would appear likely that the three magnocellular orexinergic clusters reported herein for the giraffe and harbour porpoise are homologous to those previously reported in other mammalian species. With the addition of the parvocellular cluster, it would appear that the nuclear organization of the orexinergic system reaches its greatest level of complexity (based on the number of identifiable subdivisions) in the Cetartiodactyla. This finding may of course have significant functional implications that are worth exploring, maybe not in giraffe and harbour porpoises, but within species, such as sheep and pigs, that are more readily accessible for laboratory investigations.
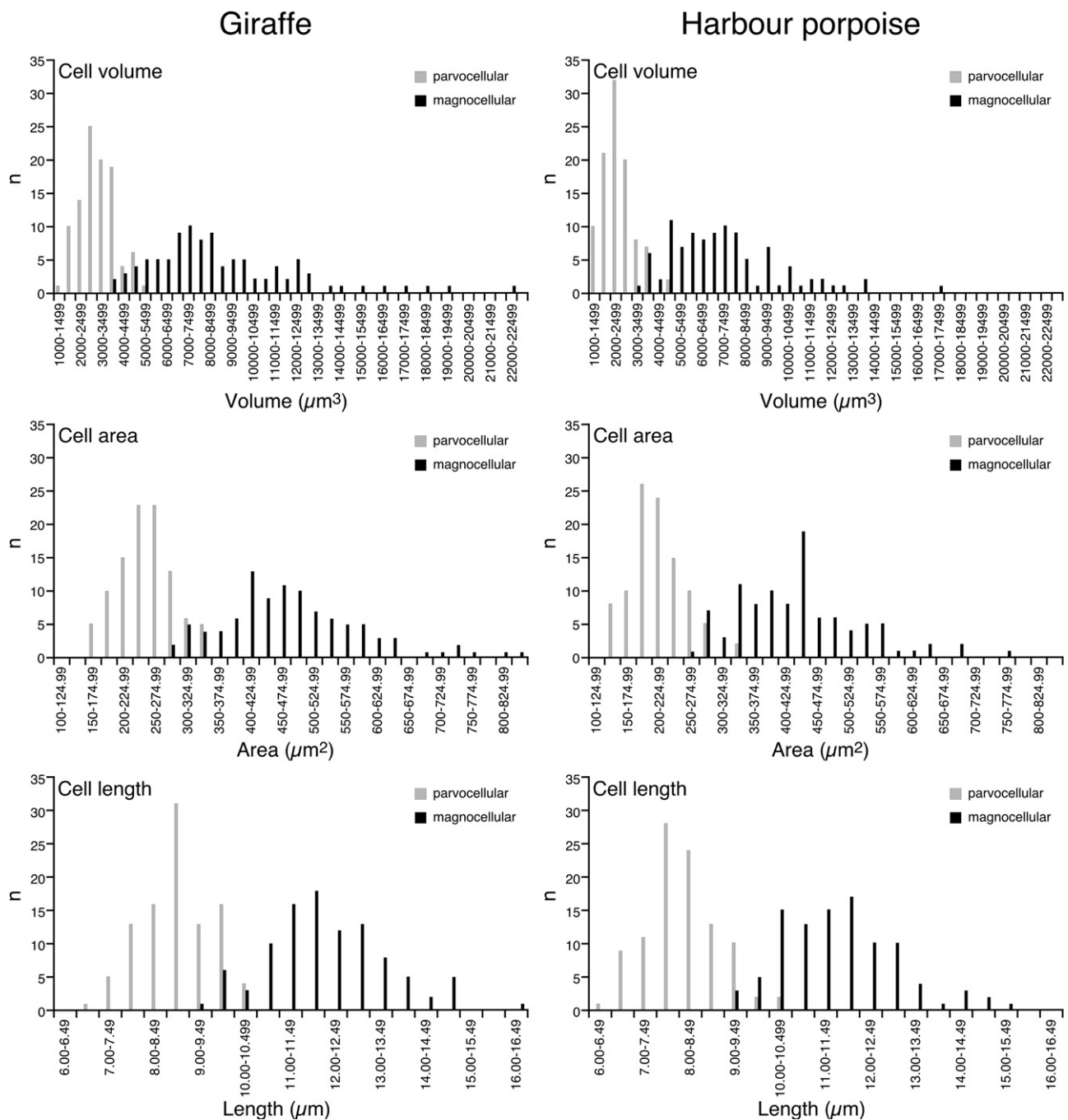
Fig. 8. Graphs showing the frequency distribution of orexinergic cellular volumes (upper two graphs), areas (middle two graphs) and lengths (lower two graphs) in the sampled giraffes (left column of graphs) and harbour porpoises (right column of graphs). As can be seen for all three parameters, the distinction between parvocellular and magnocellular orexinergic neurons is quite clear, despite a small overlap in the distributions.

4.2. Function of the Cetartiodactyla parvocellular orexinergic system

The orexinergic system has been implicated in a vast range of functions, including the control of the sleep-wake cycle, some respiratory functions, feeding and satiety, neuroendocrine and some locomotory functions (Sakurai et al., 1998; Ida et al., 1999; Mintz et al., 2001; Ferguson and Samson, 2003; Zeitzer et al., 2003; Kirouac et al., 2005; Takakusaki et al., 2005). The three magnocellular orexinergic clusters reported herein are likely to be homologous to the generalized orexinergic system found in many other mammals (see above) and, based on this assumption, we could likely conclude that their functional properties are similar to that seen in other mammals. Despite this, the

observation of a Cetartiodactyl specific parvocellular nucleus in the medial hypothalamus indicates a broader function associated with the orexinergic system in the Cetartiodactyls. The medial hypothalamus is generally associated with the initiation of copulatory, aggressive and appetitive behaviours. In this sense, having small orexinergic neurons, that appear to form local circuits based on the high density of the orexinergic terminal network in the paraventricular hypothalamus of the Cetartiodactyls studied in the current paper, the appetitive behaviours are probably of most importance to the Cetartiodactyla. Giraffe are browsers and have access to food higher in nutrients than grazers, which allows them to eat less food per day (about 30 kg) (Kingdon, 2003); however, the appetitive drive in order to find this amount of nutrition should

be strong. It is possible that an increase in appetitive drive in the giraffe results at least in part from the activity of the parvocellular orexinergic cluster. The harbour porpoise, in contrast to the giraffe, survives on a high quality, nutrient rich food source, eating between 5 and 10% of its body mass per day (Santos and Pierce, 2003); however, the life history of the harbour porpoise is an energetically demanding one (Santos and Pierce, 2003) and they also require a great deal of fuel to overcome thermal demands (Manger, 2006). Thus, the parvocellular orexinergic cluster may also drive an increase in appetitive behaviour in the harbour porpoises. The proposed role of parvocellular neurons acting to increase appetitive drive can be tested by determining the presence of these orexinergic neurons in non-Cetartiodactyl herbivores, or other mammals requiring high nutritional intake. This may also be tested physiologically in, for example, sheep, by administering agonists and antagonists to alter orexinergic activity within the parvocellular cluster. Determining the function of this parvocellular group would be of broad interest to our understanding of mammals with a demanding nutritional/appetitive lifestyle.

4.3. Stereological analysis of the Cetartiodactyla orexinergic system

The stereological analysis of the orexinergic system undertaken in the current study revealed three results of importance: (1) the cluster of orexinergic neurons in the medial hypothalamus is indeed substantially smaller than those located in the other orexinergic clusters (see above); (2) despite having similar brain masses, the number of orexinergic neurons in both parvocellular and magnocellular divisions were higher in the harbour porpoise than the giraffe; and (3) despite having a lower number of neurons, the overall size (volume, area and length) of both parvocellular and magnocellular orexinergic neurons was greater in the giraffe than the harbour porpoise. As detailed in the results, the harbour porpoise has approximately 21 000 orexinergic neurons (~51% parvocellular, ~49% magnocellular) whereas the giraffe has approximately 15 000 orexinergic neurons (~51% parvocellular and ~49% magnocellular). Thus, while the proportions of parvocellular to magnocellular are similar, the harbour porpoise has approximately 6000 additional orexinergic neurons despite having a brain slightly smaller in mass (~30 g less) than the giraffe. The increase in orexinergic neuronal number cannot be assigned to one cell type, rather it appears that, in comparison to the giraffe, the orexinergic system of the harbour porpoise has undergone a quantitative increase. The hyperplasia of the parvocellular cluster may relate to a greater need for appetitive drive in the harbour porpoise as compared to the giraffe due to the different environmental conditions the two species face (see above). In contrast, the increased number of orexinergic magnocellular neurons may rather be related to differences in the sleep-wake cycle in the two species. As mentioned earlier, the giraffe has approximately 5 h of bihemispheric sleep per night, including clear periods of REM sleep (Tobler and Schwierin, 1996), whereas the unihemispherically/alternating sleeping harbour porpoise has approximately 7 h of slow wave sleep per hemisphere per day and no REM sleep (Mukhametov and Polyakova, 1981; Lyamin et al., 2008). Given the clear relationship to arousal of the orexinergic neurons in other mammals, the need for a consistent level of arousal in the harbour porpoise, i.e. there is no period when both hemispheres show slow wave activity, and the lack of REM, it is possible that the supranumerary magnocellular orexinergic neurons within the brain of the harbour porpoise are driving this increased need for arousal of the brain, or half the brain during unihemispheric slow wave sleep. This possibility is, however, somewhat offset by our other finding of larger neurons in the giraffe than the harbour porpoise, whereby the larger neurons may be able to support a greater axonal terminal network per neuron

than the smaller neurons. It would thus be of interest to examine whether, say in the cerebral cortex, the density of the orexinergic terminal network differs between the giraffe and the harbour porpoise. We can speculate that if arousal is the key factor increasing the number of orexinergic neurons in the harbour porpoise, then the terminal networks of the orexinergic system with the cerebral cortex of the harbour porpoise should have a higher density than that seen in the giraffe (or more generally, this should be the case in cetaceans compared with terrestrial artiodactyls). On the other hand, it should be considered that in the giraffe living on the savannah with predatory animals there is a demand for an intense arousal in wakefulness which may be accomplished through an increased formation of OxA+ terminal networks driving arousal. It may be that the giraffe and the harbour porpoise have found two different ways to increase arousal and appetite, namely through hypertrophy (giraffe) and hyperplasia (harbour portoise) of the magnocellular and parvocellular orexinergic neuronal terminal networks. As another alternative, the large size of the orexinergic neurons in the giraffe may be related to the fact that they need to maintain the long orexinergic axons that project to the spinal cord (van den Pol, 1999), which is an extremely long structure in the giraffe (Badlangana et al., 2007b). Clearly there is still a great deal of work to be done to determine the functional correlates of the novel findings presented in this study, but the proposed observations will be useful to our understanding of both sleep-wake, arousal and appetitive mechanisms across mammalian species and specifically in the Cetartiodactyla.

References

Badlangana, N.L., Bhagwandin, A., Fuxe, K., Manger, P.R., 2007a. Distribution and morphology of putative catecholaminergic and serotonergic neurons in the medulla oblongata of a sub-adult giraffe, *Giraffa camelopardalis*. Journal of Chemical Neuroanatomy 34, 69–79.

Badlangana, N.L., Bhagwandin, A., Fuxe, K., Manger, P.R., 2007b. Observations on the giraffe central nervous system related to the corticospinal tract, motor cortex and spinal cord: what difference does a long neck make? Neuroscience 148, 522–534.

Badlangana, N.L., Adams, J.W., Manger, P.R., 2009. The giraffe (*Giraffa camelopardalis*) cervical vertebral column: a heuristic example in understanding evolutionary processes? Zoological Journal of the Linnean Society 155, 736–757.

Baumann, C.R., Bassetti, C.L., 2005. Hypocretins (orexins): clinical impact of the discovery of a neurotransmitter. Sleep Medicine Reviews 9, 253–268.

Bhagwandin, A., Fuxe, K., Bennett, N.C., Manger, P.R., 2011a. Distribtuion of orexinergic neurons and their terminal networks in the brains of two species of African mole rats. Journal of Chemical Neuroanatomy 41, 32–42.

Bhagwandin, A., Gravett, N., Hemingway, J., Oosthuizen, M.K., Bennett, N.C., Siegel, J.M., Manger, P.R., 2011b. Orexinergic neuron numbers in three species of African mole rats with rhythmic and arrhythmic chronotypes. Neuroscience 199, 153–165.

Bux, F., Bhagwandin, A., Fuxe, K., Manger, P.R., 2010. Organization of cholinergic, putative catecholaminergic and serotonergic nuclei in the diencephalon, midbrain and pons of sub-adult male giraffes. Journal of Chemical Neuroanatomy 39, 189–203.

Ettrup, K.S., Srensen, J.S., Bjarkam, C.R., 2010. The anatomy of the Göttingen minipig hypothalamus. Journal of Chemical Neuroanatomy 39, 151–165.

Fabris, C., Cozzi, B., Hay-Schmidt, A., Naver, B., Moller, M., 2004. Demonstration of an orexinergic central innervaton of the pineal gland of the pig. Journal of Comparative Neurology 471, 113–127.

Ferguson, A.V., Samson, W.K., 2003. The orexin/hypocretin system: a critical regulator of neuroendocrine and autonomic function. Frontiers in Neuroendocrinology 24, 141–150.

Gallyas, F., 1979. Silver staining of myelin by means of physical development. Neurological Research 1, 203–209.

Gravett, N., Bhagwandin, A., Fuxe, K., Manger, P.R., 2011. Distribution of orexin-A immunoreactive neurons and their terminal networks in the brain of the rock hyrax, *Procavia capansis*. Journal of Chemical Neuroanatomy 41, 86–96.

Gundersen, H.J., 1988. The nucleator. Journal of Microscopy 151, 3–21.

Hof, P.R., Van der Gucht, E., 2007. Structure of the cerebral cortex of the humpback whale, *Megaptera novaeangliae* (Cetacea, Mysticeti, Balaeopteridae). Anatomical Record 290, 1–31.

Hof, P.R., Chanis, R., Marino, L., 2005. Cortical complexity in cetacean brains. Anatomical Record A 287, 1142–1152.

Holm, S., 1979. A simple sequentially rejective multiple test procedure. Scandinavian Journal of Statistics 6, 65–70.

Ida, T., Nakahara, K., Katayama, T., Murakami, N., Nakazato, M., 1999. Effect of lateral cerebroventricular injection of the appetite-stimulating neuropeptide, orexin and neuropeptide Y, on the various behavioural activities of rats. Brain Research 821, 526–529.

Iqbal, J., Pompolo, S., Sakurai, T., Clarke, I.J., 2001. Evidence that orexine-containing neurons provide direct input to gonadotrophin-releasing hormone neurones in the ovine hypothalamus. Journal of Neuroendocrinology 13, 1033–1041.

Khorooshi, R.M., Klingenspor, M., 2005. Neuronal distribution of melanin-concentrating hormone, cocaine- and amphetamine regulated transcript and orexin B in the brain of the Djungarian hamster (*Phodopus sungorus*). Journal of Chemical Neuroanatomy 29, 137–148.

Kingdon, J., 2003. Kingdon Field Guide to African Mammals. Princeton University Press, Princeton, USA.

Kirouac, G., Parson, M.P., Li, S., 2005. Orexin (hypocretin) innervation of the paraventricular nucleus of the thalamus. Brain Research 1059, 179–188.

Kruger, J.-L., Dell, L.-A., Pettigrew, J.D., Manger, P.R., 2010. Cellular location and major terminal networks of the orexinergic system in the brains of five microchiropteran species. Journal of Chemical Neuroanatomy 40, 256–262.

O'Leary, M.A., 1999. Parsimony analysis of total evidence from extinct and extant taxa and the Cetacean-Artiodactyl question (Mammalia, Ungulata). Cladistics 15, 315–330.

Lyamin, O.I., Manger, P.R., Ridgway, S.H., Muhametov, L.M., Siegel, J.M., 2008. Cetacean sleep: an unusual form of mammalian sleep. Neuroscience and Biobehavioral Reviews 32, 1451–1484.

Manger, P.R., 2005. Establishing order at the systems level in mammalian brain evolution. Brain Research Bulletin 66, 282–289.

Manger, P.R., 2006. An examination of cetacean brain structure with a novel hypothesis correlating thermogenesis to the evolution of a big brain. Biological Review 81, 293–338.

Manger, P.R., Ridgway, S.H., Siegel, J.M., 2003. The locus coeruleus complex of the bottlenose dolphin (*Tursiops truncatus*) as revealed by tyrosine hydroxylase immunohistochemistry. Journal of Sleep Research 12, 149–155.

Manger, P.R., Fuxe, K., Ridgway, S.H., Siegel, J.M., 2004. The distribution and morphological characteristics of catecholamine cells in the diencephalon and midbrain of the bottlenose dolphin (*Tursiops truncatus*). Brain, Behavior and Evolution 64, 42–60.

Manger, P.R., Pillay, P., Maseko, B.C., Bhagwandin, A., Gravett, N., Moon, D.J., Jillani, N.E., Hemingway, J., 2009. Acquisition of the brain of the African elephant (*Loxodonta africana*): perfusion-fixation and dissection. Journal of Neuroscience Methods 179, 16–21.

McGranaghan, P.A., Piggins, H.D., 2001. Orexin A-like immunoreactivity in the hypothalamus and thalamus of the Syrian hamster (*Mesocricetus auratus*) and Siberain hamster (*Phodopus sungorus*), with special reference to circadian structures. Brain Research 904, 234–244.

McGregor, R., Wu, M.-F., Barber, G., Ramanthan, L., Siegel, J.M., 2011. Highly specific role of hypocretin (orexin) neurons: differential activation as a function of diurnal phase, operant reinforcement vs. operant avoidance and light level. Journal of Neuroscience 31, 15455–15467.

Mintz, E.M., van Den Pol, A.N., Casano, A.A., Albers, H.E., 2001. Distribution of hypocretin (orexin) immunoreactivity in the central nervous system of Syrian hamsters (*Mesocricetus auratus*). Journal of Chemical Neuroanatomy 21, 225–238.

Mukhametov, L.M., Polyakova, I.G., 1981. EEG investigation of sleep in porpoises (*Phocoena phocoena*). Journal of Higher Nervous Activity 31, 333–339.

Nixon, J.P., Smale, L., 2007. A comparative analysis of the distribution of immunoreactive orexin A and B in the brain of nocturnal and diurnal rodents. Behavioral Brain Function 3, 28.

Oelschläger, H.H., 2008. The dolphin brain – a challenge for synthetic neurobiology. Brain Research Bulletin 75, 450–459.

Peyron, C., Tighe, D.K., van den Pol, A.N., de Lecea, L., Heller, H.C., Sutcliffe, J.G., Kilduff, T.S., 1998. Neurons containing hypocretin (orexin) project to multiple neuronal systems. Journal of Neuroscience 18, 9996–10015.

Price, S.A., Bininda-Emonds, O.R., Gittleman, J.L., 2005. A complete phylogeny of the whales, dolphins and even-toed hoofed mammals (Cetartiodactyla). Biological Review 80, 445–473.

Sakurai, T., Amemiya, A., Ishii, M., Matsuzaki, I., Chemelli, R.M., Tanaka, H., Williams, S.C., Richardson, J.A., Kozlowski, G.P., Wilson, S., Arch, J.R., Buckingham, R.E., Haynes, A.C., Carr, S.A., Annan, R.S., McNulty, D.E., Liu, W.S., Terret, J.A., Elshourbagy, N.A., Bergsma, D.J., Yanagisawa, M., 1998. Orexins and orexin receptors: a family of hypothalamic neuropeptides and G protein-coupled receptors that regulate feeding behavior. Cell 92, 573–585.

Santos, M.B., Pierce, G.J., 2003. The diet of harbour porpoise (*Phocoena phocoena*) in the northeast Atlantic. Oceanogrphy and Marine Biology Annual Review 41, 355–390.

Shimamura, M., Yasue, H., Ohshima, K., Abe, H., Kato, H., Kishiro, T., Goto, M., Munechika, I., Okada, N., 1997. Molecular evidence from retroposons that whales form a clade within even-toed ungulates. Nature 388, 666–670.

Sokal, R.R., Rohlf, F.J., 1998. Biometry, 3rd ed. W.H. Freeman and Company, New York.

Spinazzi, R., Andries, P.G., Rossi, G.P., Nussdorfer, G.G., 2006. Orexins in the regulation of the hypothalamic–pituitary–adrenal axis. Pharmacological Review 58, 46–57.

Takakusaki, K., Takahashi, K., Saitoh, K., Harada, H., Okumura, T., Kayama, Y., Koyama, Y., 2005. Orexinergic projections to the cat midbrain mediate alternation of emotional behavioural states from locomotion to cataplexy. Journal of Physiology 568, 1003–1020.

Tobler, I., Schwierin, B., 1996. Behavioural sleep in the giraffe (*Giraffa camelopardalis*) in a zoological garden. Journal of Sleep Research 5, 21–32.

van den Pol, A.N., 1999. Hypothalamic hypocretin (orexin): robust innervation of the spinal cord. Journal of Neuroscience 19, 3171–3182.

Vidal, L., Blanchard, J., Morin, L.P., 2005. Hypothalamic and zona incerta neurons expressing hypocretin, but not melanin concentrating hormone, project to the hamster intergeniculate leaflet. Neuroscience 134, 1081–1090.

Wagner, D., Salin-Pascual, R., Greco, M.A., Shiromani, P.J., 2000. Distribution of hypocretin-containing neurons in the lateral hypothalamus and c-fos-immunoreactive neurons in the VLPO. Sleep Research Online 3, 35–42.

Zeitzer, J.M., Buckmaster, C.L., Parker, K.J., Hauck, C.M., Lyons, D.M., Mignot, E., 2003. Circadian and homeostatic regulation of hypocretin in a primate model: implications for the consolidation of wakefulness. Journal of Neuroscience 23, 3555–3560.